JOURNAL OF MATERIALS SCIENCE **34** (1999) 1017–1023

Grain growth in alumina-silica fibers

G. G. TIBBETTS, A. K. SACHDEV, A. M. WIMS, V. FRANETOVIC
General Motors Research and Development Center, 30500 Mound Road, Warren, MI, 48009-9055

Alumina-silica fibers, produced by air blowing a melt of 47 wt % alumina and 53 wt % silica, are initially amorphous, but may be heat treated to convert them into mullite and increase crystallite size. On heating to near 1000 °C, an exothermic phase transition abruptly produces mullite X-ray peaks. Further 1 hour heat treatments gradually sharpen these peaks until a minimum peak width is reached near 1600 °C. Scherrer calculations of crystallite size show that the mullite crystallites formed near 1000 °C are about 13 nm in diameter; these regions grow to about 100 nm after 1 hour at 1600 °C.

1. Introduction

Alumina-silica fibers are of interest for composite fabrication, since they are relatively inexpensive, yet possess good high temperature tensile strength and low coefficient of thermal expansion [1]. In this work Kaowool fibers made by Thermal Ceramics of Augusta, GA, were studied. Their process blasts a several mm thick stream of molten kaolin ($Al_2O_3 \cdot 2SiO_2$) with a supersonic air jet. The shearing forces arising from this violent collision produce fibers averaging 2.5 μm in diameter. Moreover, the rapid cooling of the melt makes these fibers amorphous, i.e. no peaks are visible on the X-ray diffractometer scan.

Previous studies of mullite crystallite growth in alumina-silica ceramics were hampered by the unavailability of amorphous starting material. Fahrenholtz and Smith [2] showed that the addition of Na (from 0 to 2 wt %) to mullite precursor gels increased the grain size developed after heat treatment. They concluded that Na addition created a stable intergranular glassy phase which added porosity and nourished crystallite growth because of its low viscosity.

In this report we will describe grain growth in mullite starting with an initial material which is truly amorphous. We shall see that the amorphous silica second phase and the fiber impurities control grain growth.

2. Experimental

Bulk samples of the fibers were obtained by suspending the fibers in water, collecting them on a filter, and drying the resulting porous mass. The resulting "preforms" may be used in fabricating composites.

X-ray diffractometer scans were obtained under the following conditions: Preform specimens were 2 mm thick slices mounted on plastic plate holders. A Siemens Corp. Model D-5000 automated diffractometer equipped with a carbon monochromater and an automated sample changer was used for all measurements. X-rays were produced by a copper target operated at 40 kV and 30 mA. The collimator included three apertures, including a 0.05° detector aperture, and a 0.15° diffracted beam aperture. After establishing that all of the large X-ray peaks obtained were due to the mullite lattice, only the region about the largest singlet peak, (121), was generally recorded. Angular measurements were made over a 2θ range from 35° to 45° in 0.05° steps with a count time of 240 s/step. In order to extract the Full Width at Half Maximum (FWHM), the $K_{\alpha 2}$ contribution was subtracted and the data was fitted to a Pearson VII function (a generalized Lorentz function).

To obtain X-ray diffraction scans of the loose fibers, the fibers were mounted on a low-background sample plate made from a single quartz crystal cut 6° from the *c*-axis. Angular measurements were made over a 2θ range from 10° to 80° in 0.05° steps with a count time of 1 s/step.

Thermal Ceramics Inc. sampled four different lots of amorphous Kaowool fibers which were, in principle, made by identical techniques. Variations among these lots could stem from slight composition differences, variability in the "blowing" process, or sampling irregularities. The lots were labeled "calibration" (from 1991), and, "March 8", "August 25", and "November 16" (all from 1993). From each lot, preforms were made with 15% by volume fibers using standard techniques and heat treated at the GM R&D Center to various temperatures for various durations. Heating and cooling rates for all samples were 7.5 °C/min.

Differential thermal analysis was performed on a Netzsch STA 409. A difference signal obtained from thermocouples placed both in the sample crucible and an alumina powder reference crucible were recorded while heating at 10 °C/min in an atmosphere of Ar.

3. Results

3.1. Chemistry

Table I lists a semi-quantitative chemical analysis obtained by inductively coupled plasma on the raw Kaowool fibers. The fibers are relatively pure, with the primary impurities being Na, Zn, Ca, Fe, Ti, and Mg. The manufacturer targets the composition of these fibers at 47.5 wt % Al_2O_3 and 52.5 wt % SiO_2, making

TABLE I Chemical analysis of alumina-silica fibers

Element	Concentration (wt %)	Thermal ceramics target (wt %)
Si	26.1 ± 1	24.5
Al	23.3 ± 1	25.1
Na	0.13	
Zn	0.1	
Ca	0.08	
Fe	0.07	
Ti	0.01	
Mg	0.008	

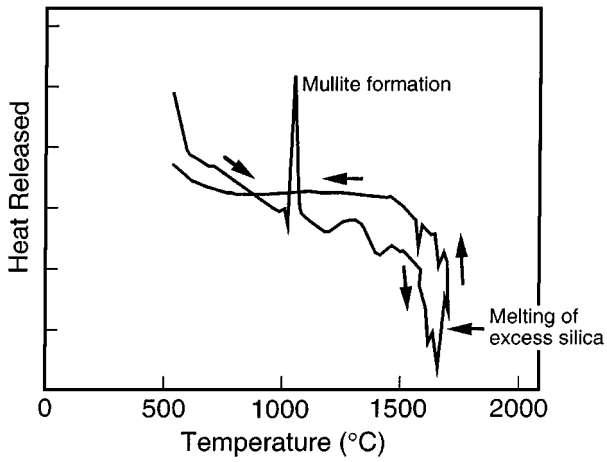

Figure 1 Differential Thermal Analysis of amorphous alumina-silica fibers heated in argon at 50 °C/min. The heating curve shows the mullite transformation slightly above 1000 ° C, while the cooling curve does not.

them richer in silica than the mullite composition of $3Al_2O_3{\cdot}2SiO_2$. Our semi-quantitative results show Al to be marginally less abundant and Si to be marginally more abundant than the target values, listed also in Table I.

Fig. 1 shows a differential thermal analysis curve for the raw fibers; it shows that during heating the sample releases a small amount of energy near 1000 °C in a very sharp transition. Comparing this data with X-ray results (Fig. 2), which show that mullite peaks first appear at 1000 °C, convinces us that this peak is associated with mullite formation:

$$3(Al_2O_3{\cdot}2SiO_2)\,\text{(amorphous)} \rightarrow 3Al_2O_3{\cdot}$$

$$2SiO_2\,\text{(mullite)} + 4SiO_2\,\text{(amorphous silica)}$$

Tabular data shows a small positive (+5.44 kcal/mol [3]) enthalpy required to form mullite from α-alumina and quartz, but this number could become negative for amorphous forms of these reactants. Further heating shows minor heat release which may be associated with growth of the crystallite grains. Over 1500 °C, the excess silica inclusions begin to melt, absorbing energy. The sharp peak near 1000 °C is not recorded during the cooling curve, affirming our conclusion that this peak corresponds to a structural change.

3.2. X-ray diffraction

Fig. 2 compares the X-ray diffraction patterns for the loose heat treated fibers with the as-received material.

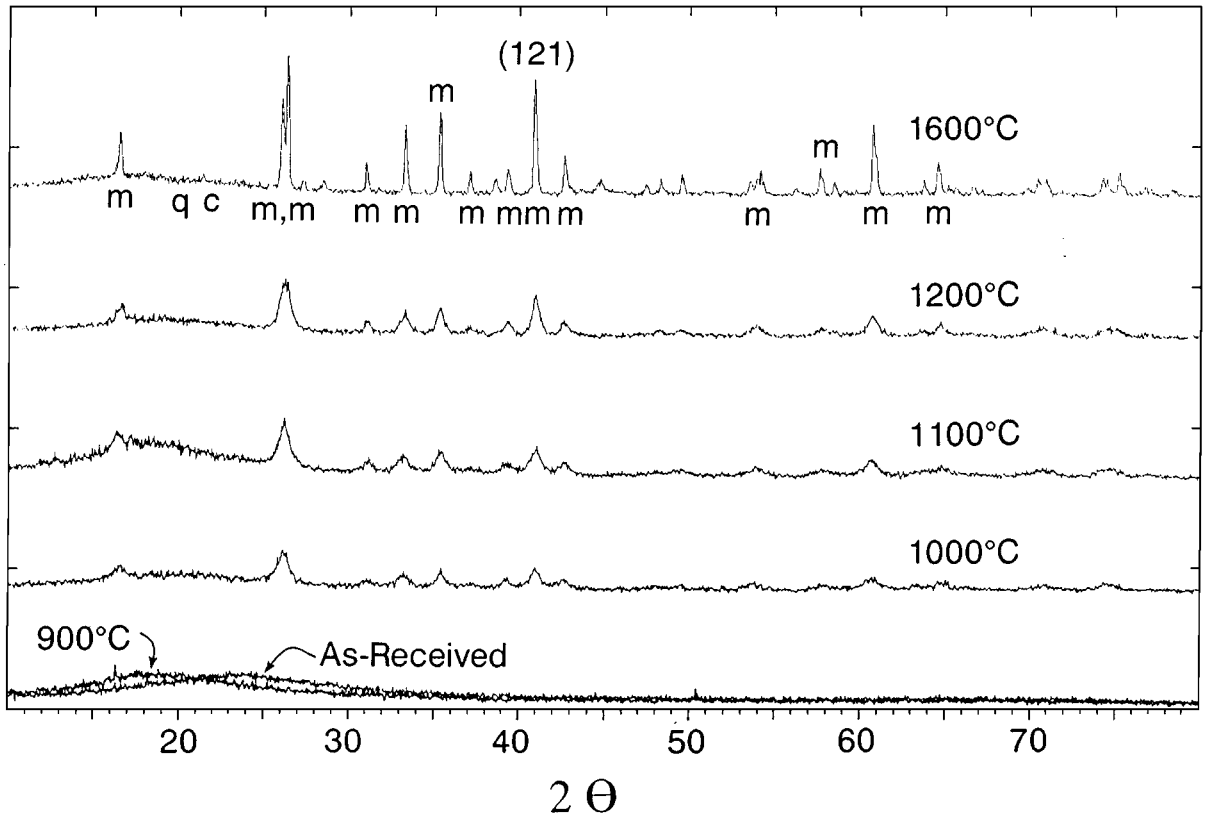

Figure 2 X-ray diffraction scans for alumina-silica fibers heat-treated at various temperatures for 1 hour. Positions of mullite peaks are marked with an "m"; the expected position of the largest cristobalite peak is marked with a "c", while the expected position of the largest quartz peak is marked with a "q".

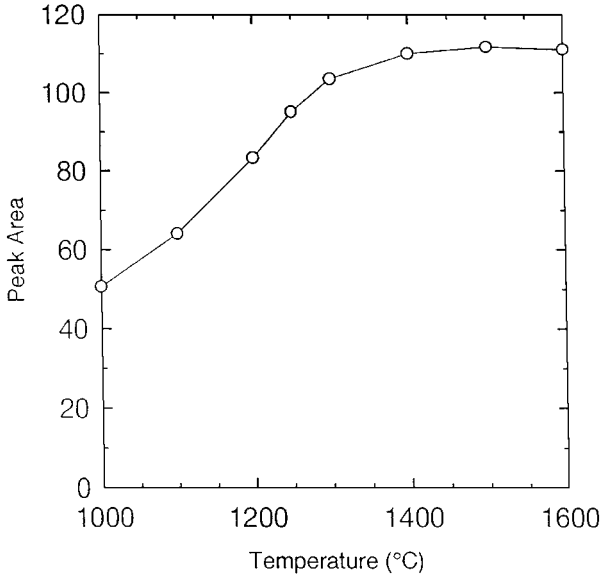

Figure 3 X-ray peak areas under the largest ((120) + (210)) peak plotted as a function of 1 hour heat treatment temperature for Kaowool fibers.

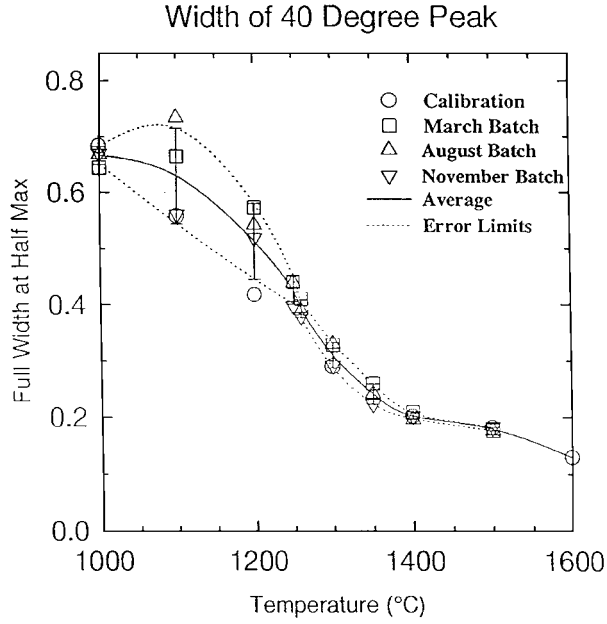

Figure 4 Full width at half maximum (FWHM) of (121) peaks of mullite for alumina-silica fibers from 4 different batches heat treated for 1 hour at various temperatures. The full line is a spline curve drawn through the average values, while the dotted lines are drawn through the average values ± the standard deviations.

Note that heating to 900 °C changed the pattern very little, but definite peaks emerged after heating to 1000 °C. These peaks grew and sharpened with temperature until 1600 °C was reached. The major peaks due to mullite are marked with an "m"; because of the complexity of the mullite structure the smaller mullite peaks above 45° are not marked. For comparison, the primary cristobalite (c) and quartz (q) peak positions are also marked; it is clear that any peaks from these reflections are very small. The 1600 °C sample is thus principally comprised of mullite; despite the fact that stoichiometry indicates that silica should be in excess, neither cristobalite nor quartz can be detected. This probably indicates that the excess silica is amorphous.

It is interesting to compare increases in X-ray peak area with decreases in peak width as heat treatment temperature increases. Fig. 3 illustrates how the integrated area of the largest ((120) + (210)) peak near 26° varies with heat treatment temperature. At 1300 °C, for example, it is only 8% below its maximum value.

In contrast, the full width of the X-ray peaks at half of their maximum amplitude decreases much more slowly as a function of temperature. Fig. 4 shows the FWHM of the 40° (121) peak for pieces cut from all four samples described above and heat treated for 1 hour to various temperatures. As Fig. 4 shows, the FWHM decreases markedly for the samples heat treated to high temperatures for 1 hour. However, the average half width near 1300 °C is over 150% larger than the value at 1600 °C.

Fig. 4 shows that above 1400 °C, all four batches surveyed gave identical FWHM values. As the heat treatment temperature decreased, values of FWHM became more and more divergent until the differences once again became small at 1000 °C. Error bars were calculated from the standard deviations of the available data at each temperature while the full line was drawn through the average values.

The data in Fig. 4 shows that the March and August batch give consistently higher FWHMs, while the November batch is generally close to the calibration values. This implies that the latter two batches are intrinsically more completely crystallized than the former two. Subsequent heat treatments apparently do not destroy this difference.

Variations in X-ray linewidth in ceramics are due to the presence of crystallites smaller than 0.1 μm or strains in the material [4]. Judging from the fact that the position of the (121) X-ray peak varies little with heat treatment temperature (Fig. 5), we infer that there are no significant macrostrains within the ceramic. Microstrains present in the as-grown amorphous material are probably quickly relaxed above 1000 °C.

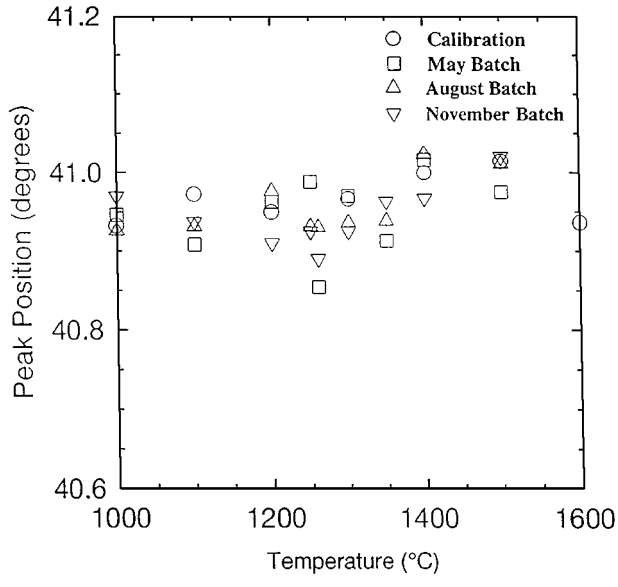

Figure 5 Position of (121) peak center determined for the 4 sample sets used in Fig. 4.

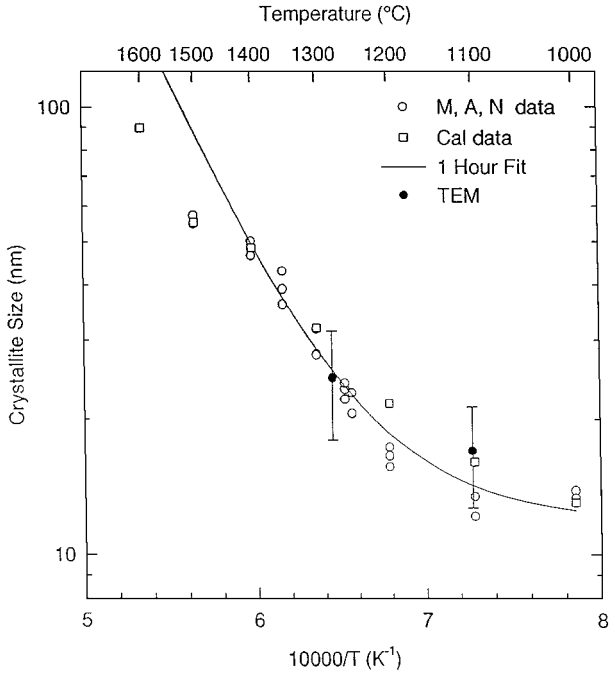

Figure 6 Crystallite size determined from the Scherrer equation applied to the (121) peaks of four different fiber samples heat treated for 1 hour to various temperatures. Data from the "March", "August", and "November" batches are shown as open circles, while the "calibration" batch data are shown as open squares. The least squares fit to Equation 1 is the full line.

3.3. Crystallite size

Using the above data on the full width at half maximum (FWHM) of the (121) X-ray peaks of fiber samples we may utilize the Scherrer equation [4] to determine the average mullite crystallite size, *d*.

$$d = \frac{0.94\lambda}{\cos\theta\sqrt{FWHM^2 - FWHM_0^2}} \qquad (1)$$

Here θ is the diffraction angle, λ is the X-ray wavelength, FWHM is the observed angular breadth of the mullite peak, and $FWHM_0$ is the breadth (0.0846°) of a single crystal diffracted line (indicating the instrumental broadening). Converting the above FWHM values of various alumina-silica fiber preforms to crystallite size gives the data in Fig. 6. Data points for the 4 different preform batches subjected to 1 hour heat treatments at various temperatures are shown. The lowest temperature data shown (at $10000/T = 7.85$), representing a heat treatment at 1000 °C, shows nucleation of crystallites about 13 nm in diameter. A slight increase in temperature, to 1100 °C, has little effect in increasing crystallite size. Ultimately, however, the logarithm of crystallite size increased linearly with $10000/T$, indicating a temperature activated process. The solid line which is drawn in Fig. 6 to fit the data ignores the two highest temperature data points at 1600 °C ($10000/T = 5.34$) and 1500 °C ($10000/T = 5.54$); in this region the X-ray linewidth

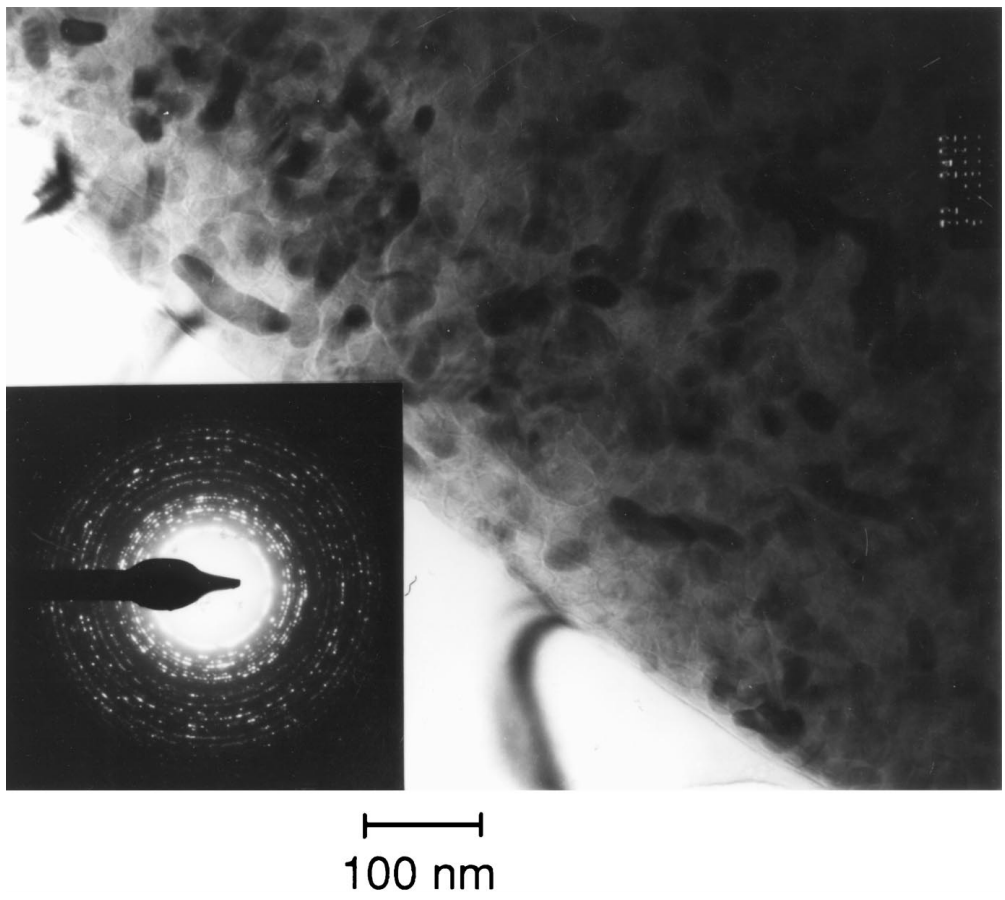

Figure 7 Transmission electron micrograph of thinned sample of alumina-silica fibers heat treated to 1278 °C. The inset is a selected area diffraction pattern of the 1278 °C sample.

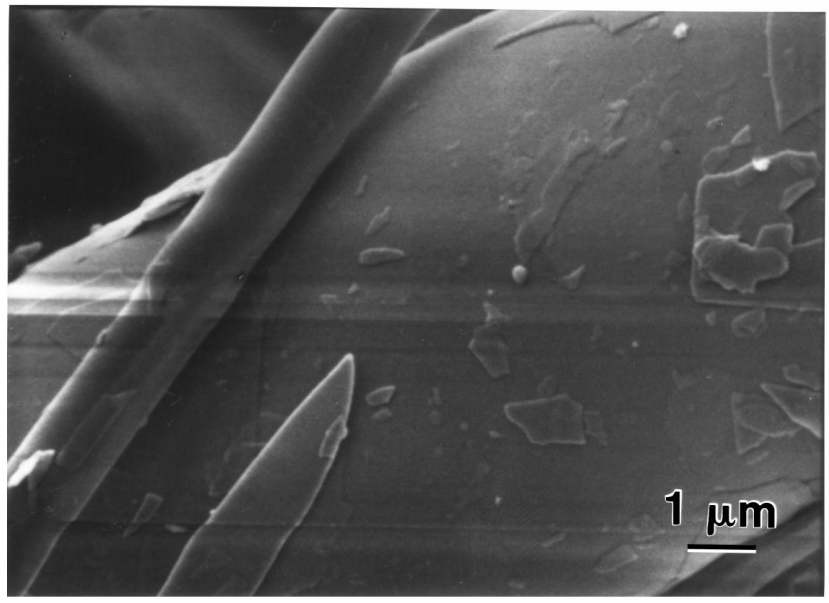

a

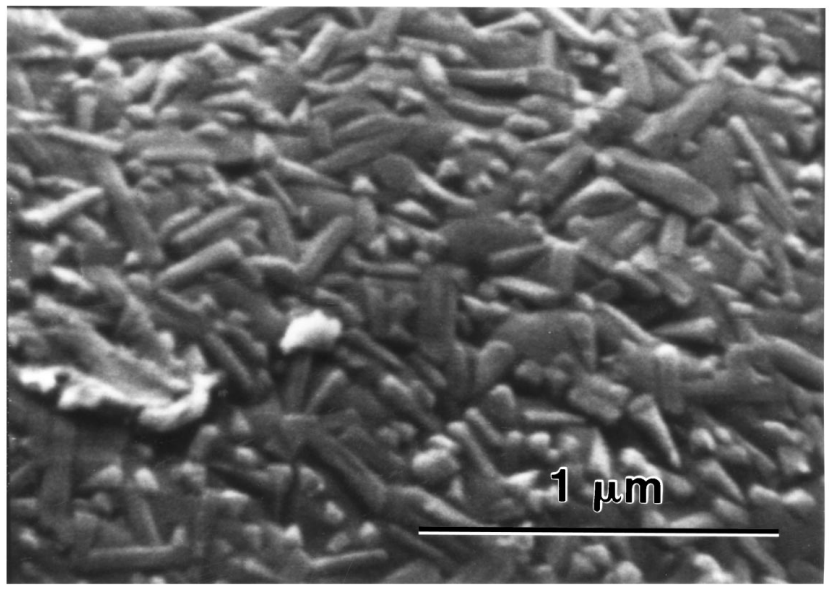

b

Figure 8 Scanning electron microscope images of alumina-silica fiber surfaces heated to (a) 1260 °C, and (b) 1500 °C for 1 hour.

approaches the instrumental broadening and errors in determination of crystallite size become large as the denominator of Equation 1 becomes small. The equation represented by the solid line,

$$d = d_0 + d_1 \, \mathrm{e}^{-(E/RT)}, \tag{2}$$

is fitted to the data to obtain d_0 as 12 nm, near the size of the initial crystallite, d_1 as a constant, and E as an activation energy (176 kJ/mol), where R is the gas constant and T is the absolute temperature.

Fig. 7 shows a transmission electron micrograph of a thinned section of a fiber heat treated at 1278 °C. The corresponding selected area diffraction pattern (inset) shows a ringlike pattern of discrete points, characteristic of a material composed of fine polycrystals. These micrographs make it clear that, even at this modest temperature, a substantial portion of the entire volume is crystallized, so that many crystallites are competing for the remaining amorphous material. An averaged measurement of the (two dimensional) minor diameter of crystallites shown is 24.7 ± 6.8 nm, and is shown as the solid circle on Fig. 6, in good agreement with the Scherrer equation crystallite determinations and the least squares fit. A second data point made from a similar sample heat treated at 1100 °C is also plotted in Fig. 6.

Even scanning electron microscope images are sufficient to resolve the 1500 °C crystallites. Fig. 8a shows how smooth the surface of a fiber is after heat treatment to 1000 °C, while Fig. 8b shows the large crystallites which form on the surface after heat treatment to 1500 °C.

The growth of crystallites with time is displayed in Fig. 9 for three different growth temperatures. Only the three dated batches were used, as the original "calibration" batch was unavailable. For all three temperatures shown, the logarithm of crystallite diameter

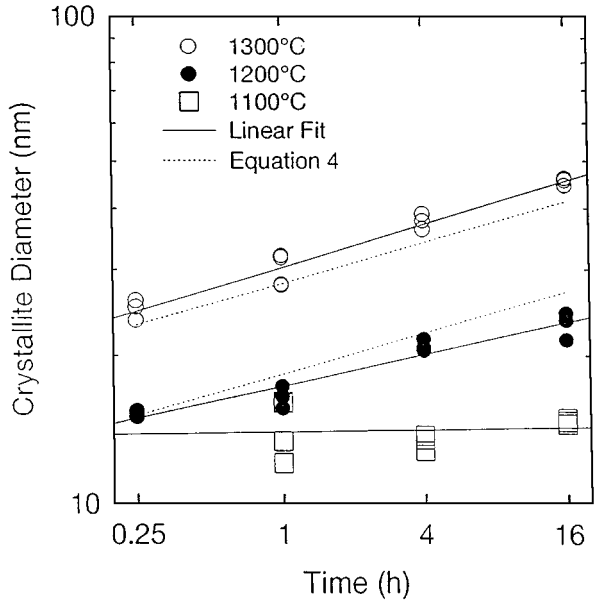

Figure 9 Crystallite diameter determined from the Scherrer equation from (121) X-ray peak as a function of heat treatment duration for 3 different temperatures. The full lines are the least squares linear fits to the data. The dotted lines are calculated from Equation 4.

varies linearly with the logarithm of time in accord with the frequently cited equation [5],

$$d = d_2 t^n, \tag{3}$$

where n may be determined by the slope of each line. The slope of the two higher temperature plots clearly shows crystallite growth, but the 1100 °C data shows no growth. The values for n determined from the slopes of the two higher temperature curves are 0.15 and 0.11. These numbers are all considerably smaller than theoretical values, which range from 1/3 for diffusional control [6] to 1/2 for interfacial reaction control [7]. It is clear that while a temperature of 1100 °C is high enough for nucleation to occur, it is too low for significant crystallite growth.

Equations 2 and 3 are actually special cases of a more elaborate equation expressing d in terms of both time and temperature. A simple equation incorporating both dependencies is

$$d = \left(d_0 + d_1 \, \mathrm{e}^{-(E/RT)}\right) t^n. \tag{4}$$

Using the activation energy E of 176 kJ/mol, an average value of n of 0.14, and the interpolated crystallite size from the "1 hour fit" curve of Fig. 6 provides an estimate of crystallite size as a function of time for different temperatures. These estimates are shown as dotted lines in Fig. 9 and are reasonable approximations to the actual least squares fits.

For small values of time, Equations 3 and 4 may not be very good approximations. To allow for a finite size critical nucleus d_0 at $t = 0$, some authors [5] have used expressions of the type

$$d^{1/n} = d_0^{1/n} + kt \tag{5}$$

instead of Equation 3. For values of d far above d_0, both Equations 3 and 5 will yield similar results, but 3 extrapolates to a critical nucleus of 0 size. Therefore, the size of the critical nucleus becomes a key matter. Nucleation studies in glass oxide systems [8] have reported nuclei near 3 nm in size, much smaller than the 12 nm obtained by fitting our data, perhaps indicating some crystallite growth before our X-ray measurements can detect crystal structure.

4. Discussion

Most previous studies of recrystallization have used pure metals where, typically, n (in Equation 3) is in the range 0.4–0.5, in agreement with a host of calculations which attempt to model the problem of coalescent recrystallization with various approximations [5]. Impurities have been shown to decrease the rate and increase the apparent activation energy of recrystallization in metals [9]. For example, in a study of Mn in Ti, n was found to be 0.26 and 0.22 for the two metals [10]. In another study, activation energies for the coarsening kinetics of Ag particles in Ni [11] were found to lie between 132 and 322 kJ/mol, values which lie between that for grain boundary and volume diffusion in Ni.

As we have shown, these alumina-silica fibers are comprised of a mixture of mullite and amorphous silica phases, with a high concentrations of impurities; they are a more complex mixture than is usually studied, although some results on two-phase ceramics have been reported. A study of grain growth kinetics in alumina-zirconia ceramics yielded n values between 0.25 and 0.33, coupled with E values of 700–865 kJ/mol [12]. This very large activation energy was found to be consistent with boundary-diffusion-controlled grain growth and in agreement with values measured in creep and superplastic deformation experiments.

Our results on the crystallization of these alumina-silica fibers obtained from both microscopy and X-ray diffraction are in agreement. While the as-produced fibers are amorphous, heating them to 1000 °C, slightly greater than the temperature at which mullite formation is observed by differential thermal analysis, causes nucleation of abundant 13 nm crystallites. The activation energy for crystallite growth is closer to values normally found in metals rather than values observed in zirconia-toughened alumina [12]. The rate of crystallite growth with time is slower than observed in pure materials, but these alumina-silica fibers contains silica and impurity phases which could impede crystallite growth. It is reasonable to attribute the low rate of grain growth to these phases. Indeed, Soni *et al*. [13] have stated in a study of Saffil fibers (96% alumina, 4% silica) that the silica is added to prevent coarsening of the Al_2O_3 grains by segregating to the grain boundaries. Hence, even though the rate of crystallite growth with time in these alumina-silica fibers is exceptionally low because they are a complex multi-phase material, the activation energy of grain growth is also relatively low. This low activation energy implies that grain growth proceeds by a mechanism more efficient than boundary

diffusion control; it is more consistent with coalescent recrystallization.

Acknowledgements

Special thanks are due to Howard K. Lee for much help with heat treatments and X-ray diffractometry. We would also like to thank S. Willett and R. Hall for technical help and S. Katz for helpful discussions. We also acknowledge the differential thermal analysis experiments of J. Bommarito and semi-quantitative chemical analysis by D. Esch.

References

1. "Kaowool Ceramic Fiber Products," Product Bulletin 002 5M, Thermal Ceramics, Inc., Augusta, GA, 1992.
2. W. G. FAHRENHOLTZ and D. M. SMITH, *J. Amer. Ceram. Soc*. **77** (1994) 1377.
3. J. L. HOLM and O. J. KLEPPA, *J. Phys. Chem*. **70** (1966) 1690.
4. B. D. CULLITY, "Elements of X-Ray Diffraction" (Addison-Wesley, Reading, MA, 1978) p. 284.
5. M. P. ANDERSON, D. J. SRILOVITZ, G. S. GREST and P. S. SAHHI, *Acta Metall*. **32** (1984) 782.
6. I. M. LIFSCHITZ and V. V. SLYOZOV, *J. Phys. Chem. Solids* **19** (1961) 35.
7. C. WAGNER, *Z. Elektrochem*. **65** (1961) 581.
8. P. F. JAMES, in "Advances in Ceramics," Vol. 4, edited by J. H. Simmons, D. R. Uhlmann and G. H. Beall (American Ceramic Society, Columbus, OH, 1982) p. 1.
9. O. DIMITROV, R. FROMAGEAU and C. DIMITRIOV, in "Recrystallization of Metallic Materials," edited by F. Hassner (Riederer Verlag, Stuttgart, 1978) p. 111.
10. G. GREWAL and S. ANKEM, *Acta Metall. Mater*. **38** (1990) 1607.
11. S. C. YANG, G. T. HIGGENS and P. NASH, *Mater. Sci. Technol*. **8** (1992) 10.
12. K. B. ALEXANDER, P. F. BECHER, S. B. WATERS and A. BLEIR, *J. Amer. Ceram. Soc*. **77** (1994) 939.
13. K. K. SONI, H .G. KANG, P. S. GRANT, B. CANTOR, A. G. ADRIAENS, K. L. GARIVOV, R. MOGILEVSKY, R. LEVI-SITTI, M. W. TSENG and D. B. WILLIAMS, *J. Microscopy* **177** (1995) 414.

Received 4 November 1997
and accepted 9 October 1998